

Cr³⁺ DOPED YTTRIUM GALLIUM GARNET FOR PHOSPHOR-CONVERSION LIGHT EMITTING DIODES

A. Zabiliūtė-Karaliūnė^a, H. Dapkus^a, R.P. Petrauskas^b, S. Butkutė^b, A. Žukauskas^a, and
A. Kareiva^b

^a Institute of Applied Research, Vilnius University, Saulėtekio 9-III, LT-10222 Vilnius, Lithuania

^b Department of General and Inorganic Chemistry, Vilnius University, Naugarduko 24, LT-03225 Vilnius, Lithuania
E-mail: akvile.zabiliute@tmi.vu.lt

Received 22 May 2015; revised 2 July 2015; accepted 29 September 2015

In this work Y₃Ga₅O₁₂ doped with 8.7 mol% Cr³⁺ (YGG:Cr) far-red phosphor pellets calcined at 1000, 1200, 1300, and 1400 °C temperatures were synthesized by a simple and low cost sol–gel method. The YGG:Cr pellets were investigated using X-ray diffraction (XRD) and scanning electron microscopy (SEM) and the luminescent properties were studied by measuring diffuse reflection, photoluminescence (PL), PL excitation (PLE) and internal quantum efficiency (QE). The XRD and SEM results have shown that the material becomes more crystalline, uniform and less porous for higher calcination temperatures. XRD results have also shown that the material becomes strained due to the doping with Cr³⁺ ions for the calcination temperature of 1400 °C. The diffuse reflection and PLE spectra have shown three absorption and excitation bands in the UV, blue and red spectral regions. PL was characterized by a broad band in the far-red spectral region that peaked at about 711 nm. QE has shown a strong dependence on the calcination temperature. Furthermore, using the previously synthesized YGG:Cr phosphor powder and a commercial blue InGaN LED, a far-red–blue phosphor converted LED (pcLED) lamp was designed and characterized. Blue–far-red pcLEDs could be used in greenhouses in order to meet the photophysiological needs of plants.

Keywords: Light-emitting diodes, phosphors, photoluminescence, far-red light, sol–gel

PACS: 78.55.Hx, 81.20.Fw, 85.60.Jb

1. Introduction

Plant cultivation in greenhouses with artificial lighting is an important technology since it enables to grow plants during any time of a year at any latitude. It also saves land in densely populated areas by developing vertical farming [1]. Nowadays high pressure sodium, metal halide, fluorescent, and incandescent lamps are mostly used for this application [2, 3]. However, solid-state lighting seems to be more attractive since it can be spectrally matched with the absorption spectra of plant photopigments thus producing less waste light, has a long lifetime, is efficient, robust, mercury-free, and needs a lower voltage supply which is safer [4]. Light emitting diodes (LEDs) also allow achieving higher productivity and nutritional quality of plants due to the fact that the spectral power distribution (SPD) of LEDs can be tailored to optimally meet the physiological needs of plants [3, 5]. It was shown that using LED facilities radish, lettuce, wheat, strawberries, chrysanthemums and other plants were successfully grown [2, 5–8].

There are three main photophysiological processes in plants: phototropism which is responsible for the movement of plants, photosynthesis which supplies plants with necessary carbohydrates, and photomorphogenesis which is responsible for the development of plants that require blue (400–500 nm), red (620–680 nm) and far-red (700–760 nm) light, respectively [9]. The blue and red components can be provided by high quality and efficient InGaN and AlGaInP LEDs, respectively. However, AlGaAs LEDs that emit light in the far-red spectral region are sensitive to humidity and temperature variations and for this reason degrade fast in the greenhouse environment [6]. A solution to this problem could be a phosphor converted LED (pcLED) composed of a blue InGaN LED and a far-red phosphor converter. Phosphor for this purpose should be characterized by a broad photoluminescence (PL) band in the far-red spectral region, in order to match the absorption spectrum of the photopigment phytochrome which controls the process of photomorphogenesis in plants [9]. Also it should have a PL excitation (PLE) peak in the blue spectral

region in order to be excited by an efficient blue LED. The phosphor also should be resistant to humid environment and temperature variations and have a long lifetime. Most of the far-red phosphors are excited by UV light (e. g. $\text{Ca}_3\text{MgSi}_2\text{O}_8:\text{Eu}^{2+}, \text{Mn}^{2+}, \text{LiAlO}_2:\text{Fe}^{3+}, \text{CaS}:\text{Yb}$) or are unstable in water (e. g. $\text{CaGa}_2\text{S}_4:\text{Mn}^{2+}$) [10]. Phosphor materials satisfying the requirements given above could be gallium garnets doped with trivalent chromium (Cr^{3+}). Cr^{3+} has 3 electrons in the d orbital which are not screened so the PL band position and width strongly depend on the crystal field and are described by Tanabe–Sugano diagrams [11, 12]. The gallium atom has a suitable size that creates the right strength crystal field in the lattice so the PL is mostly due to the ${}^4\text{T}_2 \rightarrow {}^4\text{A}_2$ transition and is characterized by a broad band in the far-red spectral region [12, 13]. PL properties of ceramic and crystalline gallium garnets doped with Cr^{3+} were investigated previously [13–16]. However, in none of this research the values of internal quantum efficiency (QE) are presented which is a very important property of phosphors for LED applications. For this reason, using a simple and low-cost sol–gel method we have previously synthesized and investigated various powder (gadolinium, gadolinium scandium, yttrium and lutetium) gallium garnets calcined at different temperatures and doped with different Cr^{3+} concentrations [17]. The results have shown that the most promising material was yttrium gallium garnet $\text{Y}_3\text{Ga}_5\text{O}_{12}:\text{Cr}^{3+}$ (YGG:Cr) 8 mol% calcined at 1300 °C temperature. The material was characterized by PLE in the blue spectral region, a broad PL band in the far-red spectral region, and 46% QE.

In this work, YGG:Cr pellets were synthesized by a sol–gel method in order to test whether the pellets exhibit better PL properties than powder. For this reason morphological (X-ray diffraction (XRD), scanning electron microscopy (SEM)) and luminescent properties (PL, PLE, and QE) of YGG:Cr 8.7 mol% phosphor pellets, calcined at the temperatures between 1000 °C and 1400 °C were measured. Furthermore, using the YGG:Cr phosphor powder described in Ref. [17] and a blue InGaN LED, a blue–far-red solid state lamp for greenhouse lighting was designed and its spectral properties such as photon flux and the efficiency of blue-to-far-red light conversion were measured.

2. Experimental details

2.1. Preparation and characterization of YGG pellets

$\text{Y}_3\text{Ga}_5\text{O}_{12}$ (YGG) doped with 8.7 mol% of Cr^{3+} (YGG:Cr) samples were synthesized via a sol–gel combustion method. Y_2O_3 , Ga_2O_3 and $\text{Cr}(\text{NO}_3)_3 \cdot 9\text{H}_2\text{O}$ were used as starting materials and tris(hydroxymethyl)ami-

nomethane (TRIS) was used as a complexing agent and fuel for the self-initiating combustion process. Metal oxides were dissolved in concentrated HNO_3 . Thermogravimetric analysis was used to estimate the amount of water for crystallization in $\text{Cr}(\text{NO}_3)_3 \cdot x\text{H}_2\text{O}$. Aqueous solutions of Y^{3+} , Ga^{3+} and Cr^{3+} with a desired molar ratio were mixed together and the necessary amount of TRIS was added. The gel formation takes around 1 h at 60–75 °C with constant mixing in a covered beaker. TRIS initiates a spontaneous self-combustion process when the gel is completely dried. The obtained very crumbly ash-like powders were heated at 800 °C for 5 h for complete removal of the residues of organic matter. The resulting powders were pressed into pellets that were heated for 10 h at 1000, 1100, 1200, 1300 and 1400 °C with a heating rate of 3 °C/min.

XRD analysis was performed using a diffractometer (Rigaku MiniFlex II) that was working in the Bragg–Brentano ($\theta/2\theta$) geometry. The data were collected within the 2θ angle between 10° and 90° at a scan speed of 10°/min using the $\text{CuK}\alpha$ line ($\lambda = 1.54060 \text{ \AA}$). The morphology of the samples was characterized using a SEM (Hitachi SU-70).

Diffuse reflection spectra were measured using a spectrometer with an integrating sphere (Perkin Elmer Lambda 950, Spectralon white standard). The spectra were recorded between 200 and 850 nm. The PLE and PL measurements were performed using a fluorescence spectrometer (Perkin Elmer LS55). PLE was measured in the range between 200 and 700 nm while monitoring PL at 711 nm. PL was measured between 600 and 900 nm upon 440 nm excitation. PL QE was measured using an integrating sphere (Sphere Optics, Spectralon white standard) and a spectrometer (Hamamatsu PMA-12). An incandescent lamp and a monochromator set at 440 nm were used for the excitation. Using this method, the PL spectra are measured in three configurations: when the sphere is empty, when the sphere is with the sample inside, but with the excitation light focused to the inner wall of the sphere and when the light is focused to the sample. Using the spectral data, the value of QE is calculated. The detailed explanation of this method is given by J. C. de Mello [18].

2.2. Prototype far-red LED lamp

Since phosphor pellets still cause technological difficulties while designing a light converter, a pcLED based blue–far-red lamp was designed using the far-red YGG phosphor powder doped with 8 mol% Cr^{3+} and calcined at a 1300 °C temperature that was synthesized by a sol–gel method at the Department of Inorganic Chemistry, Vilnius University [17].

A commercial lamp case was used as a housing and a Philips Lumileds Rebel Royal Blue (peak wavelength 452 nm) InGaN LED was used for the blue light component. The blue-to-far-red light converter was made of sanitary silicone and YGG:Cr phosphor mixture placed in a polymethylmetacrilate (PMMA) case. The mixture contained 5.7 wt% of phosphor powder and was 1.5 mm thick. The picture of the blue–far-red pLED lamp prototype and its scheme are shown in Fig. 1(a) and (b), respectively.

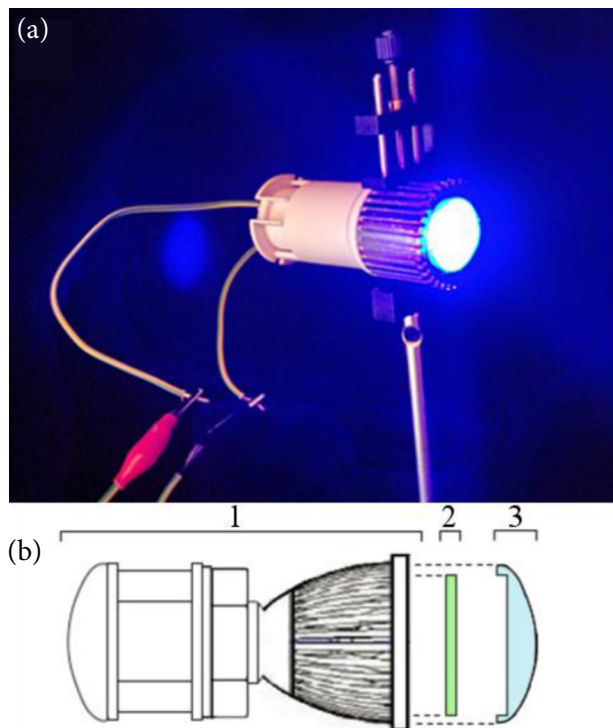


Fig. 1. (a) The prototype of the pLED lamp with two spectral components meeting the photophysiological needs of plants; (b) a scheme of the blue–far-red pLED lamp; here 1 is the housing of the lamp, 2 is the YGG:Cr powder phosphor-silicone converter, 3 is the lens.

3. Results and discussion

3.1. Characterization of YGG pellets

Figure 2 presents XRD patterns of the pellets heated between 1000 and 1400 °C. All measured patterns have a good fit with the standardized pattern of $Y_3Ga_5O_{12}$ (PDF-2 (ICDD) 00-043-0512) depicted as columns at the bottom of Fig. 2. Table 1 shows the calculated full width at half maximum (FWHM) values for the most intensive XRD diffractograms peaks of sintered pellets. As it is seen in Table 1, the FWHM values of the peaks corresponding to

the pellet calcined at 1000 °C are largest and in general they become smaller for higher calcination temperatures. This means that the crystallinity of the samples calcined at higher temperatures increases. However, a slight broadening of FWHM is observed for the pellets calcined at 1200 and 1400 °C temperatures which could be caused by strains and microstrains at the crystal unit cell in higher crystalline sample due to the doping with Cr^{3+} ions. It is known that when the crystallites are small (usually smaller than $\sim 1 \mu m$) and/or they are strained, the resultant Bragg peak widths may increase substantially [19].

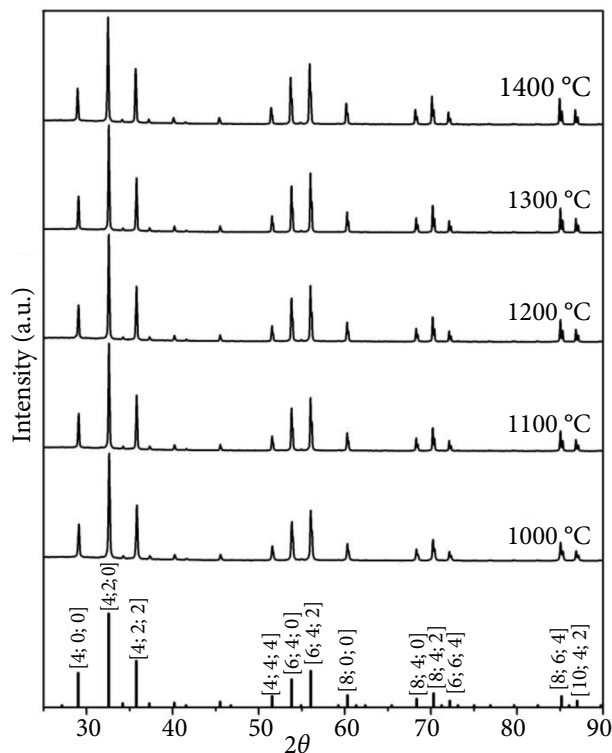


Fig. 2. XRD pattern of the YGG:Cr 8.7 mol% phosphor pellets calcined at different temperatures. Column lines correspond to the standardized $Y_3Ga_5O_{12}$ XRD pattern (PDF-2 (ICDD) 00-043-0512).

The morphology of YGG:Cr samples can be evaluated by SEM. Figure 3 shows the SEM images of the YGG:Cr pellets calcined at the temperatures from 1200 to 1400 °C. It is seen in the figure that for higher calcination temperatures the material becomes less porous, more uniform and that the crystallites forming the pellets grow in size for higher calcination temperatures.

Figure 4 shows the diffuse reflection spectra of the YGG:Cr pellets calcined at different temperatures. It is seen from the figure that all samples are characterized by a strong absorption in the UV region caused

Table 1. Calculated FWHM values for the most intensive XRD diffractograms peaks of sintered pellets.

PDF # 00-043-0512		FWHM				
2θ	[h; k; l]	1000 °C	1100 °C	1200 °C	1300 °C	1400 °C
29.12	[4; 0; 0]	0.1704	0.1456	0.1508	0.1394	0.1503
32.64	[4; 2; 0]	0.1724	0.1490	0.1506	0.1425	0.1515
35.85	[4; 2; 2]	0.1789	0.1549	0.1575	0.1489	0.1571
51.60	[4; 4; 4]	0.2051	0.1303	0.1769	0.1677	0.1841
53.88	[6; 4; 0]	0.1573	0.1201	0.1338	0.1210	0.1385
56.08	[6; 4; 2]	0.1628	0.1259	0.1353	0.1241	0.1342
60.34	[8; 0; 0]	0.1499	0.1195	0.1268	0.1173	0.1283
68.38	[8; 4; 0]	0.1429	0.1162	0.1178	0.1123	0.1245
70.31	[8; 4; 2]	0.1447	0.1130	0.1134	0.1065	0.1182
72.22	[6; 6; 4]	0.1405	0.1144	0.1127	0.1055	0.1167
85.17	[8; 6; 4]	0.1543	0.1180	0.1131	0.1071	0.1133
86.98	[10; 4; 2]	0.2000	0.1600	0.2000	0.2000	0.2000

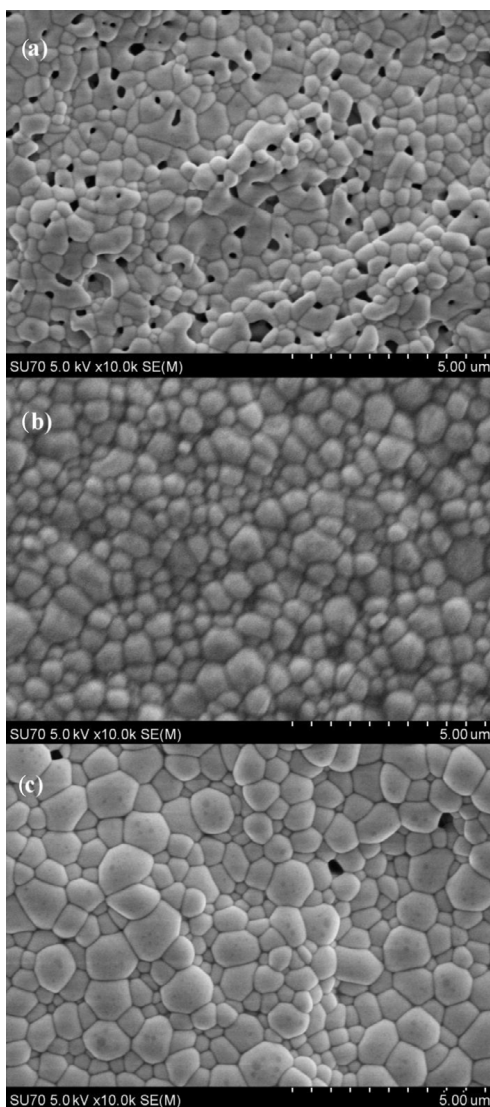


Fig. 3. SEM pictures of the YGG:Cr 8.7 mol% phosphor pellets calcined at different temperatures: (a) 1200 °C, (b) 1300 °C, (c) 1400 °C. It is seen that for higher calcination temperatures the material becomes less porous and the crystallites grow in size.

by the ${}^4A_2 \rightarrow {}^4T_1$ transition [20]. The samples calcined at the temperatures between 1200 and 1400 °C also show absorption in the blue (400–500 nm) and red (570–650 nm) spectral ranges which are caused by the ${}^4A_2 \rightarrow {}^4T_1$ and ${}^4A_2 \rightarrow {}^4T_2$ transitions in Cr^{3+} , respectively [12, 13, 20]. However, the figure also shows that the absorption in the pellet calcined at 1000 °C is significantly lower, the edge of the UV reflectivity spectrum is slightly shifted to lower wavelengths, the absorption in the red spectral range is reduced and in the blue spectral range it is almost gone. This can be explained by the fact that 1000 °C temperature is not high enough to completely remove the organic residues and form high quality crystallites, what well coincides with the XRD results above.

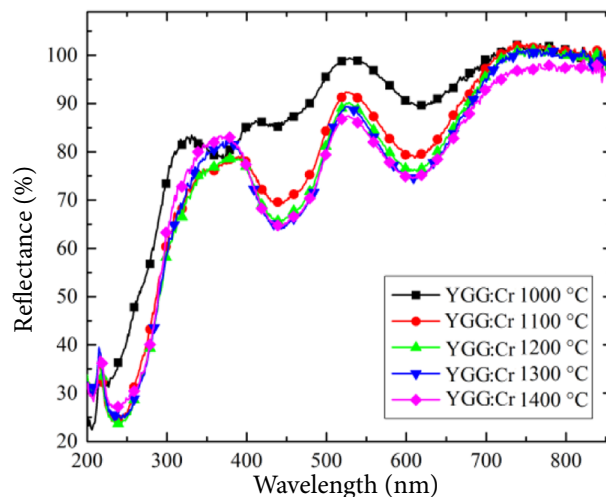


Fig. 4. Diffuse reflection spectra of the YGG:Cr 8.7 mol% phosphor pellets calcined at the temperatures between 1000 and 1400 °C. Absorption in the UV and blue regions is caused by the ${}^4A_2 \rightarrow {}^4T_1$ transition and in the red region by the ${}^4A_2 \rightarrow {}^4T_2$ transition.

The PLE spectra of the YGG:Cr pellets are depicted in Fig. 5. The presented PLE spectra have three bands in the UV, blue and red regions that peak at around 214, 439 and 605 nm, respectively. The excitation in UV and blue spectral regions occurs due to the ${}^4A_2 \rightarrow {}^4T_1$ transition and that in the red spectral region is due to the ${}^4A_2 \rightarrow {}^4T_2$ transition as in the case of absorption. Figure 5 shows that in general the intensity of PLE increases for higher calcination temperatures with slight fluctuations for the samples calcined at 1100 and 1200 °C temperature and abruptly drops for the pellet calcined at 1400 °C. The PLE intensity increases due to the higher quality of crystallites that are obtained for higher calcination temperatures. However, for very high temperatures the size of crystallites increases thus increasing the reabsorption that reduces the PL intensity of the phosphor. This can be confirmed by the diffuse reflection spectra that show the absorption in the far-red region where PL takes place being higher for the pellet calcined at 1400 °C if compared to other samples.

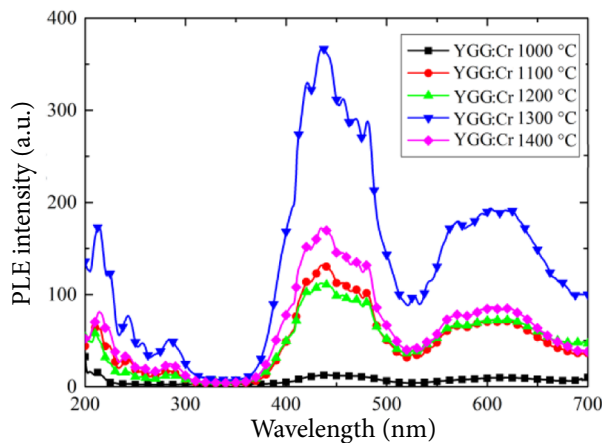


Fig. 5. PLE spectra of the YGG:Cr 8.7 mol% phosphor pellets calcined at the temperatures between 1000 and 1400 °C. PLE spectra peak in the UV, blue and red regions at around 214, 439 and 605 nm, respectively. PL was monitored at 711 nm.

The PL intensity dependence on calcination temperature is presented in Fig. 6. It is seen in the figure that PL is characterized by a broad band in the far-red region caused by the ${}^4T_2 \rightarrow {}^4A_2$ transition that peaks around 711 nm and by a narrow zero phonon R line caused by the ${}^2E \rightarrow {}^4A_2$ transition that peaks at around 693 nm [12, 13]. The tendency of PL intensity is exactly the same as for PLE: the intensity increases for higher calcination temperatures with slight fluctuations and decreases when the temperature reaches 1400 °C. The PL and PLE spectra of the YGG:Cr phosphor pellets are similar in shape

and intensity variation to the spectra of the YGG:Cr phosphor powder investigated before [17].

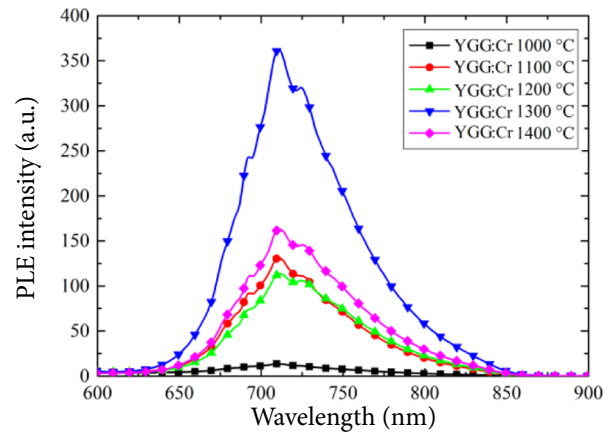


Fig. 6. PL spectra of the YGG:Cr 8.7 mol% phosphor pellets calcined at the temperatures between 1000 and 1400 °C upon 440 nm excitation. The broad PL band in the far-red region is caused by the ${}^4T_2 \rightarrow {}^4A_2$ transition and peaks at around 711 nm.

The values of internal QE are given in Table 2. It is seen that the values of QE increase for higher calcination temperature until it reaches 55% for 1300 °C calcination temperature and saturates. This value is even by 9% larger than the QE of the YGG:Cr³⁺ 8 mol% phosphor powder [17]. The growth of QE can be explained by the improvement of crystal properties of the crystallites that form the pellets, as it is seen in Fig. 3, which causes the reduction of non-radiative transitions. However, the growth of the crystallites in size increases the reabsorption, therefore the PL intensity of the pellet calcined at 1400 °C drops as discussed above. Despite that fact that pellets are more efficient than powders, the integration of pellets into the pLED lamp is still a technological challenge.

Table 2. Values of the QE of the YGG:Cr 8.7 mol% phosphor pellets and YGG:Cr 8 mol% phosphor powder [17] calcined at different temperatures.

Calcination temperature	QE of the YGG:Cr 8.7 mol% pellets	QE of the YGG:Cr 8 mol% powder [17]
1000 °C	23%	18%
1100 °C	49%	–
1200 °C	53%	–
1300 °C	55%	46%
1400 °C	55%	33%

3.2. Characterization of pcLED lamp

The spectrum of the designed pcLED lamp is presented in Fig. 7. It is seen that the SPD consists of two spectral components in the blue and far-red regions, respectively. The ratio of blue to far-red light is 4.7 and it meets the phototropic and photomorphogenetic needs of plants [9]. However, in order to completely meet the photophysiological needs of plants, the designed pcLED lamp should be combined with a red LED lamp radiating in the 620–680 nm spectral region [21]. The properties of the designed blue-to-far-red light converter are given in Table 3. The photon flux was calculated by integrating the spectrum in the ranges of 400–520 nm and 650–850 nm for blue and far-red light, respectively; the blue LED was driven by 350 mA current. Table 3 shows that the efficiency of the converter is 35%, which is a satisfactory value, since the QE of the YGG powder used was 46% [17]. The designed pcLED lamp is transferred to the Lithuanian Research Centre for Agriculture and Forestry for further research in greenhouses in order to investigate the lamp impact on plant growth.

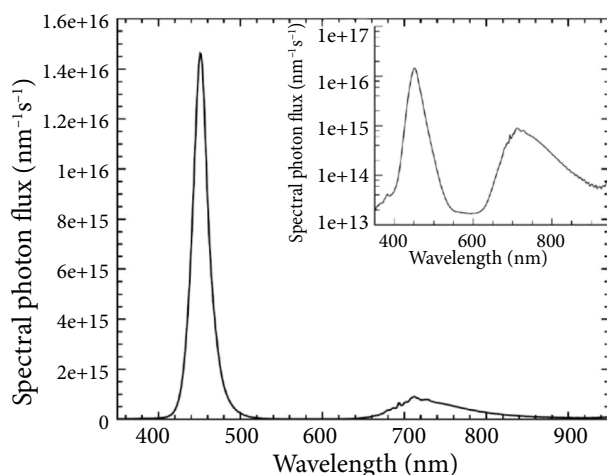


Fig. 7. The emission spectrum of the blue–far-red pcLED lamp for the plants. The inset shows the same spectrum in a logarithmic scale. The spectrum consists of two components in the blue and far-red regions that can satisfy phototropic and photomorphogenetic needs of plants.

4. Conclusions

The XRD patterns of the YGG:Cr phosphor pellets doped with 8.7 mol% of Cr³⁺ have shown that the quality of crystallites forming pellets increases with calcination temperature. The broadening of the FWHM values for the pellet calcined at 1400 °C shows that the lattice of the garnet becomes strained due to the Cr³⁺ ions. The SEM images of the samples have shown that for higher calcination temperatures material becomes less porous and crystallites grow in size. The diffuse reflection spectra of the pellets show absorption in the UV, blue and red spectral regions; these results agree with the PLE spectra that consist of three bands in the UV, blue and red spectral regions that peak at about 214, 439 and 605 nm, respectively. The intensity of PLE strongly depends on the calcination temperature and is the highest for the pellet calcined at 1300 °C temperature. The PL spectra of the samples are characterized by a broad band in the far-red spectral region and peak at about 711 nm. The PL intensity shows the same behaviour as PLE and is the highest for the pellet calcined at 1300 °C temperature. The PL intensity of the pellet calcined at 1400 °C temperature drops due to increased reabsorption which is seen in the diffuse reflection spectra and is caused by the increased size of the crystallites forming the pellet as SEM images show. QE increases with the calcination temperature of the pellets up to 55% and saturates for the calcination temperatures above 1300 °C. This value is by 9% higher than for the powder samples synthesized before which means that the phosphor pellets surpass powder and they could be exploited in far-red pcLEDs designed for horticultural applications.

The spectrum of the designed pcLED lamp consists of two components in the blue and far-red regions, respectively, with the blue to far-red photon flux ratio 4.7. The efficiency of the blue to far-red light converter made of the YGG:Cr³⁺ 8 mol% phosphor powder and sanitary silicone mixture placed in a PMMA case is 35% which is a satisfactory value for the QE of the phosphor powder of 46%. According to the measured data the designed blue–far-red pcLED lamp used with a supplementary red LED lamp could

Table 3. Spectral properties of the designed blue–far-red pcLED lamp for plants. Blue LED driving current was 350 mA.

	Photon flux
Blue component in the lamp covered by a transparent lens	2.21 $\mu\text{mol/s}$
Blue component in the lamp covered by a converter	0.64 $\mu\text{mol/s}$
Far-red component in the lamp covered by a converter	0.14 $\mu\text{mol/s}$
Sum of blue and far-red components	0.78 $\mu\text{mol/s}$
Efficiency of the converter	35%

satisfy the photophysiological needs of plants and is thus transferred to the Lithuanian Research Centre for Agriculture and Forestry for further research on plant growth in greenhouses.

Acknowledgements

The authors would like to thank prof. Živilė Lukšienė for providing equipment for the measurements of PLE and PL. This work was partly supported by the project “Promotion of Student Scientific Activities” (VP1-3.1-ŠMM-01-V-02-003) from the Research Council of Lithuania (H. Dapkus). This project is funded by the Republic of Lithuania and the European Social Fund under the 2007–2013 Human Resources Development Operational Programme’s Priority 3.

References

- [1] D. Despommier, *The Vertical Farm: Feeding the World in the 21st Century* (St. Martin’s Press, USA, 2010).
- [2] S.J. Kim, E.J. Hahn, J.W. Heo, and K.Y. Paek, Effects of LEDs on net photosynthetic rate, growth and leaf stomata of chrysanthemum plantlets in vitro. *Sci. Hortic.* **101**(1), 143–151 (2004), <http://dx.doi.org/10.1016/j.scienta.2003.10.003>
- [3] H. Shimizu, Y. Saito, H. Nakashima, J. Miyasaka, and K. Ohdoi, in: *Proceedings of the 18th IFAC World Congress*, Vol. 18 (International Federation of Automatic Control, Milano, 2011) pp. 605–609.
- [4] N. Yeh and J.-P. Chung, High-brightness LEDs – energy efficient lighting sources and their potential in indoor plant cultivation, *Renew. Sust. Energ. Rev.* **13**(8), 2175–2180 (2009), <http://dx.doi.org/10.1016/j.rser.2009.01.027>
- [5] R.C. Morrow, LED lighting in horticulture, *Hortscience* **43**(7), 1947–1950 (2008).
- [6] G. Tamulaitis, P. Duchovskis, Z. Bliznikas, K. Breivė, R. Ulinskaitė, A. Brazaitytė, A. Novičkovas, and A. Žukauskas, High-power light-emitting diode based facility for plant cultivation, *J. Phys. D* **38**(17), 3182–3187 (2005), <http://dx.doi.org/10.1088/0022-3727/38/17/020>
- [7] R.J. Bula, R.C. Morrow, T.W. Tibbitts, D.J. Barta, R.W. Ignatius, and T.S. Martin, Light-emitting diodes as a radiation source for plants, *Hortscience* **26**(2), 203–205 (1991).
- [8] C.S. Brown, A.C. Schurger, and J.C. Sager, Growth and photomorphogenesis of pepper plants under red light-emitting diodes with supplemental blue or far-red lighting, *J. Am. Soc. Hortic. Sci.* **120**(5), 808–813 (1995), <http://dx.doi.org/10.1088/0022-3727/38/17/020>
- [9] M. S. McDonald, *Photobiology of Higher Plants* (Wiley, England, 2003).
- [10] W.M. Yen and M.J. Weber, *Inorganic Phosphors: Compositions, Preparation and Optical Properties* (CRC Press, USA, 2004).
- [11] M.D. Seltzer, Interpretation of the emission spectra of trivalent chromium-doped garnet crystals using Tanabe–Sugano diagrams, *J. Chem. Educ.* **72**(10), 886–888 (1995), <http://dx.doi.org/10.1021/ed072p886>
- [12] B. Struve and G. Huber, The effect of the crystal field strength on the optical spectra of Cr³⁺ in gallium garnet laser crystals, *Appl. Phys. B* **36**(4), 195–201 (1985).
- [13] K. Petermann and G. Huber, Broad band fluorescence of transition metal doped garnets and tungstates, *J. Lumin.* **31–32**, 71–77 (1984).
- [14] M. Yamaga, A. Marshall, K.P. O’Donnell, B. Henderson, and Y. Miyazaki, Photoluminescence of Cr³⁺ ions in RF-sputtered YGG thin films, *J. Lumin.* **39**(6), 335–341 (1988).
- [15] W. Liu, Q. Zhang, L. Ding, D. Sun, J. Xiao, and S. Yin, Preparation and luminescence properties of nano-polycrystalline Cr³⁺:Lu₃Ga₅O₁₂, *Physica B* **403**(19–20), 3403–3405 (2008), <http://dx.doi.org/10.1016/j.physb.2008.04.043>
- [16] L. Kostyk, A. Luchechko, Y. Zakharko, O. Tsvetkova, and B. Kuklinski, Cr-related centers in Gd₃Ga₅O₁₂ polycrystals, *J. Lumin.* **129**(3), 312–316 (2009), <http://dx.doi.org/10.1016/j.jlumin.2008.10.011>
- [17] A. Zabaliūtė, S. Butkutė, A. Žukauskas, P. Vitta, and A. Kareiva, Sol–gel synthesized far-red chromium-doped garnet phosphors for phosphor-conversion light-emitting diodes that meet the photomorphogenetic needs of plants, *Appl. Opt.* **53**(5), 907–914 (2014), <http://dx.doi.org/10.1364/AO.53.000907>
- [18] J.C. de Mello, H.F. Wittmann, and R. Friend, An improved experimental determination of external photoluminescence quantum efficiency, *Adv. Mater.* **9**(3), 230–232 (1997), <http://dx.doi.org/10.1002/adma.19970090308>
- [19] V.K. Pecharsky and P.Y. Zavalij, *Fundamentals of Powder Diffraction and Structural Characterization of Materials*, 2nd ed. (Springer, US, 2009), <http://dx.doi.org/10.1007/978-0-387-09579-0>
- [20] G. Blasse, B.C. Grabmaier, and M. Ostertag, The afterglow mechanism of chromium-doped gadolinium gallium garnet, *J. Alloys Comp.* **200**(1–2), 17–18 (1993).
- [21] A. Žukauskas, *Puslaidininkiniai šviestukai* (Progretus, Lietuva, 2008).

Cr³⁺ LEGIRUOTAS ITRIO GALIO GRANATAS, SKIRTAS KONVERSIJOS FOSFORE ŠVIESOS DIODAMS

A. Zabaliūtė-Karaliūnė^a, H. Dapkus^a, R.P. Petrauskas^b, S. Butkutė^b, A. Žukauskas^a,
A. Kareiva^b

^a *Vilniaus universiteto Taikomųjų mokslų institutas, Vilnius, Lietuva*

^b *Vilniaus universiteto Bendrosios ir neorganinės chemijos katedra, Vilnius, Lietuva*

Santrauka

Darbe pristatomos paprastu ir nebrangiu zolių-gelių metodu susintetintos Y₃Ga₅O₁₂ fosforo tabletės, legiruotos 8,7 mol% Cr³⁺ (YGG:Cr) bei iškaitintos 1000, 1200, 1300 ir 1400 °C temperatūrose. YGG:Cr tabletės buvo ištirtos rentgeno spindulių difrakcijos (XRD) bei skenuojančios elektronų mikroskopijos (SEM) metodais, liuminescencinės savybės ištirtos išmatavus difuzinį atspindį, fotoluminescenciją (PL), PL sužadinimą (PLE) ir vidinę kvantinę išeią (QE). XRD ir SEM matavimai parodė, kad didinant iškaitinimo temperatūrą, medžiaga tampa kristališkesnė, tolydesnė ir mažiau porėta. XRD rezultatai taip pat atskleidė, kad tabletėje, iškaitintoje 1400 °C

temperatūroje, dėl legiravimo Cr³⁺ jonais atsiranda įtempimai. Difuzinio atspindžio ir PLE spektrai atskleidė tris sugerties ir sužadinimo linijas UV, mėlynoje ir raudonoje spektro srityse. PL spektrai parodė, kad PL pasižymi plačia juosta tolimoje raudonoje spektro srityje, kurios maksimumas yra ties maždaug 711 nm. Nustatyta, kad QE stipriai priklauso nuo iškaitinimo temperatūros. Be to, naudojant anksčiau susintetintus YGG:Cr fosforo miltelius ir prekinį mėlyną InGaN šviesos diodą, sukurta ir ištirta mėlyna–tolima raudona konversijos fosfore kiektakūnė lempa. Tokia lempa gali būti naudojama šiltnamiuose augalų fotofiziologiniams poreikiams tenkinti.